NASA TECHNICAL NOTE

NASA TN D-4680

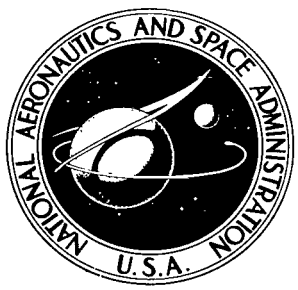

NASA TN D-4680

EXPERIMENTAL INVESTIGATION OF THE USE OF SOFT SIDE LEGS TO IMPROVE TOUCHDOWN STABILITY OF LEGGED LANDING VEHICLES

by Robert W. Herr

Langley Research Center
Langley Station, Hampton, Va.

NATIONAL AERONAUTICS AND SPACE ADMINISTRATION • WASHINGTON, D. C. • AUGUST 1968

EXPERIMENTAL INVESTIGATION OF THE USE OF SOFT SIDE LEGS TO IMPROVE TOUCHDOWN STABILITY OF LEGGED LANDING VEHICLES

By Robert W. Herr

Langley Research Center
Langley Station, Hampton, Va.

NATIONAL AERONAUTICS AND SPACE ADMINISTRATION

For sale by the Clearinghouse for Federal Scientific and Technical Information
Springfield, Virginia 22151 – CFSTI price $3.00

EXPERIMENTAL INVESTIGATION OF THE USE OF SOFT SIDE LEGS TO IMPROVE TOUCHDOWN STABILITY OF LEGGED LANDING VEHICLES

By Robert W. Herr
Langley Research Center

SUMMARY

The effectiveness of a concept to improve the landing stability of lunar-module-type vehicles has been investigated experimentally by utilizing a 1/6-scale model of an early engineering version of the lunar module. Results of landing-stability tests made with equal-force shock absorbers in all four leg assemblies are compared with results obtained with very soft shock absorbers in the side legs. This comparison indicates that landing stability can be greatly improved with the use of soft side struts if the fore and aft feet are roughly alined with the flight path at touchdown. For touchdowns at large yaw angles, the landing stability with soft side shock absorbers was at least as good as that obtained with equal-force shock absorbers.

INTRODUCTION

The Apollo lunar module will alight on four identical leg assemblies designed to attenuate the landing impact and assure landing stability. The lunar module must remain upright while landing within a specified range of ground slope and horizontal and vertical components of velocity regardless of the yaw orientation or the direction of flight with respect to the slope. The preferred yaw orientation, however, is that with two opposite feet alined with the horizontal velocity component. This orientation may result in a symmetric 1-2-1 landing mode in which one foot impacts followed by the simultaneous impact of the two adjacent feet and then the impact of the remaining foot. (The digits in the landing-mode designation signify the number of feet involved in each succeeding impact.) Some results of an early two-dimensional, rigid-body study (ref. 1) are illustrated in figure 1 and show that the stability of a four-legged vehicle is vastly improved when the side feet do not impact the surface (1-0-1 mode).

This improvement in rigid-body stability can be rationalized with the aid of the sketches in figure 1. In the left-hand sketch of the 1-2-1 mode, the uphill foot of a rigid vehicle has already impacted and the vehicle has rotated downhill about this foot until the

side feet impacted a small protuberance on the surface of the landing area. The momentum vector (mV), which passes through the instantaneous center of percussion, is seen to pass well ahead of and above the side feet. An appreciable amount of momentum is conserved because, for rigid bodies, the angular momentum after impact is equal to the moment of the momentum vector before impact. Similarly, in the right-hand sketch, it can be seen that considerable momentum is also conserved upon impact of the downhill foot since the new momentum vector passes well above the point of impact. If sufficient momentum remains after this final impact, the vehicle will rotate about the downhill foot until the center of gravity passes a point directly over the foot and the vehicle overturns. For the 1-0-1 landing mode depicted in the lower sketch, the momentum vector at second impact is seen to pass much closer to the impacting foot, and a larger loss of angular momentum results. If, in fact, the center of gravity is sufficiently low relative to the distance between the feet, the momentum vector will pass behind the downhill foot and the vehicle will have no overturning tendency regardless of the magnitude of the initial impact velocity.

For a vehicle equipped with shock absorbers it would seem reasonable to anticipate that an improvement in landing stability analogous to the superiority of the 1-0-1 rigid-body mode over the 1-2-1 rigid-body mode could be achieved by softening the shock absorbers in the side legs so that they function merely as outriggers to balance the vehicle against falling sidewise.

The experimental and analytical results reported in reference 2 show that from the standpoint of landing stability, asymmetric landings can be more critical than symmetric landings. Examination of the motions involved in these experimental three-dimensional landings indicated that softer shock absorbers in the side struts might also improve vehicle stability for this type of landing.

This paper reports the results of an experimental study to determine the effectiveness of this soft-side-leg concept. Experimentally determined stability boundaries of a 1/6-scale model with soft side struts are compared with boundaries obtained when the same model was equipped with four identical leg assemblies.

SYMBOLS

d	deflection, feet (millimeters)
F	force, pounds (newtons)
K	spring rate, pounds/foot (newtons/millimeter)

m	mass, pounds mass (kilograms)
V	velocity, feet/second (meters/second)
V_h	horizontal component of impact velocity, feet/second (meters/second)
V_v	vertical component of impact velocity, feet/second (meters/second)
α_s	cross-slope angle, degrees
σ	landing-surface slope, degrees
ψ_f	yaw angle relative to flight path, degrees
ψ_s	yaw angle relative to direction of downhill slope, degrees

APPARATUS

Model

Figure 2 is a photograph of the model used in the present investigation and in the investigation reported in reference 2. The general landing-gear configuration is one-sixth the size of an early engineering version of the lunar module (LM). Note that unlike the present LM configuration, each leg assembly of the early version resembles an inverted tripod with the secondary struts attached to the main strut near the foot. Spike feet on the model assure that the feet will stop abruptly and lift off freely when impacting the plywood landing surface. Abrupt stopping of the feet is generally more critical from a landing-stability standpoint than would be the case if the feet were allowed to slide. Pertinent dimensions of the model are given in figure 3 along with the mass and mass moment of inertia about the vehicle center of gravity. Although the LM configuration has changed since this model was constructed, parametric-trend data should be valid for the general four-legged class of landing vehicles.

In the discussion which follows, reference is made to two model configurations, one with equal-force shocks and one with soft side shocks. In the configuration with equal-force shocks, the crush force of the aluminum honeycomb energy absorbers in each of the telescoping struts was derived from the values proposed in the early engineering version of the LM from which the model was scaled. The crush force for each of the four main (upper) struts of the model was 256 pounds (1140 newtons) acting through a $4\frac{1}{2}$-inch (11.4-centimeter) stroke and a 128-pound (570-newton) force acting through a $4\frac{1}{2}$-inch (11.4-centimeter) stroke was required for each of the secondary (lower) struts. In the

configuration with soft side shocks, the crush force of the energy absorbers in each of the struts (main and secondary) of the side leg assemblies was reduced to 32 pounds (142 newtons) while the energy absorbers in the fore and aft leg assemblies remained unchanged.

With commercially available aluminum honeycomb, it was not practical to design an energy absorber with a crush force as low as 32 pounds (142 newtons). The side struts were therefore modified to use the wire energy absorber depicted in figure 4. With this device, a mild steel wire is pulled over a pulley as the strut is stroked. As the wire is bent around the pulley and again as it straightens out, virtually its entire cross section is stressed to the yield point. The force required to pull the wire over the pulley is dependent upon the diameters of the wire and the pulley and upon the stress-strain properties of the wire.

The force-deflection curve for one of the side struts equipped with the wire energy absorbers was experimentally determined and is shown in figure 5. During loading and unloading, the strut behaves as a linear elastic spring with an effective stiffness of 8570 lb/ft (125 N/mm). Although not implicit in the figure, the strut deflection associated with constant-force stroking during a typical impact was, in general, much larger than the elastic deflections associated with strut loading and unloading. The area under the return curve is a measure of the stored elastic energy available for rebound. Although this area is small, it is shown in references 2 and 3 that a small amount of elastic energy could have an appreciable effect on the computed stability boundaries of the model with equal-force shocks.

Drop Rig and Impact Platform

The model was released from a four-bar pendulum or trapeze, a part of which is visible in figure 2. The purpose of the trapeze was to launch the model in a given direction and with a controlled horizontal component of velocity. The model was attached to the trapeze by an 8-inch-diameter (20.3-centimeter) vacuum plate attached to the top of the model.

The impact platform consisted of a 10 000-pound (4536-kilogram) slab of reinforced concrete measuring 12 by 16 feet (3.66 by 4.88 meters). One end of the platform was fixed to the floor by means of a pivot arrangement and the other end could be elevated to provide the desired slope. The entire surface of the platform was covered with 3/4-inch (1.9-centimeter) plywood.

TEST PROCEDURE

In all tests reported herein, the model impacted in a horizontal attitude and with roll, pitch, and yaw rates of zero. The landing-surface slope was 10° for all tests. With

all other variables held constant, the drop height, and hence the vertical component of velocity, was varied until the stability boundary was determined to the nearest foot per second. The magnitude of the horizontal component of velocity was determined by the initial angular displacement of the pendulum. The model and trapeze swung as a unit until, at bottom dead center, the vacuum seal between them was broken and the model was allowed to drop.

RESULTS AND DISCUSSION

Vertical Landings

The experimentally determined stability profile shown in figure 6(a) was obtained by dropping the model with equal-force shocks vertically onto a 10° slope. The vertical impact velocity V_V is plotted as a function of the yaw orientation relative to the direction of downhill slope. The solid symbols denote tests in which the model overturned. The sketch at the right-hand side of figures 6 to 9 gives the orientation of the model relative to the direction of downhill slope and flight path. The black leg assemblies denote the scaled shock absorbers whereas the white leg assemblies represent the soft side shocks.

Vertical drops at $\psi_S = 0^{\circ}$ or 90° and at 45° result in two-dimensional tumbling motions referred to as 1-2-1 and 2-2 modes of overturning, respectively. In the 1-2-1 mode, the uphill foot makes initial contact with the surface and is followed, in turn, by a simultaneous impact of the two side feet and then the downhill foot. In the 2-2 mode, two uphill feet impact simultaneously followed by the simultaneous impact of the two downhill feet. Three-dimensional or asymmetric tumbling motions result when $\psi_S \neq 0^{\circ}$, 45°, or 90°.

For the configuration with equal-force shocks, the stability boundary is symmetric about $\psi_S = 45^{\circ}$. The symmetric 1-2-1 landing mode is seen to be somewhat less stable than the symmetric 2-2 landing mode and the asymmetric modes are considerably less stable than either of the symmetric modes.

The stability profile shown in figure 6(b) was obtained under conditions identical to those described for figure 6(a), with the exception that the model was equipped with soft side shocks. With 32-pound-force (142-newton) shock absorbers in each of the side struts, the model was stable at all yaw orientations and vertical velocities up to the limit of the test apparatus, i.e., 14 ft/sec (4.27 m/sec). It should be noted that the landings at 14 ft/sec (4.27 m/sec) were not just marginally stable but were extremely stable. The model appeared to squat at impact.

For the model equipped with soft side shocks, $\psi_S = 0^{\circ}$ results in a 1-2-1 landing with the hard shocks alined with the slope and $\psi_S = 90^{\circ}$ results in a 1-2-1 landing with

the soft shocks alined with the slope. All intermediate yaw angles, including 45^{o}, represent asymmetric landings.

Cross-Slope Landings

The stability of the model with equal-force shocks and the model with soft side shocks during cross-slope landings is illustrated in figures 7(a) and 7(b), respectively. The vertical component of the impact velocity V_V is plotted as a function of the cross-slope angle α_S. The cross-slope angle, illustrated in the sketch, is defined as the angle between the direction of downhill slope and the flight path. For these tests, the horizontal component of velocity V_h was 5 ft/sec (1.52 m/sec) and the vehicle yaw angle with respect to the flight path was zero. That is, the fore and aft feet were alined with the horizontal component of the velocity vector. All cross-slope angles except 0^{o} result in asymmetric postimpact motions.

Comparison of the data of figures 6(a) and 7(a) indicates, as would be expected, that the addition of horizontal velocity generally lowers the stability boundary of the model with equal-force shocks. In fact, the vertical velocity required to overturn the model approaches zero at cross-slope angles between 15^{o} and 30^{o}.

The effect of the soft side shocks on the cross-slope landing stability may be seen by comparing the results of figure 7(a) with those of figure 7(b). Again the model was stable at velocities up to at least 14 ft/sec (4.27 m/sec) regardless of the cross-slope angle.

Yawed Downhill Landings

Intuitively, it might seem that with soft energy absorbers in the side legs, it would be necessary to keep the sidewise component of velocity low to avoid rotation of the vehicle over onto the side shock absorbers. Thus, it would be necessary for the pilot to aline the fore and aft feet with the flight path. Although it is unlikely that such a restraint on maneuvering would be a problem to the pilot, if his vision is not obscured, several more landing-stability tests were made to determine the sensitivity of the 1/6-scale model to sidewise velocity.

The stability profiles shown in figures 8(a) and 8(b) were obtained by launching the model in the direction of downhill slope while varying the yaw angle relative to the flight path. In figure 8(a) the vertical component of the impact velocity of the model equipped with equal-force shocks is plotted as a function of the yaw angle ψ_f. The horizontal component of velocity was held constant at 5 ft/sec (1.52 m/sec). It is of interest to note that the model is more stable in the 1-2-1 mode ($\psi_f = 0^{o}$ and 90^{o}) than in the 2-2 mode ($\psi_f = 45^{o}$), whereas for vertical drops (fig. 6(a)) the opposite is true. Again the model is

seen to be the least stable during the asymmetric landings represented by the intermediate values $0^o < \psi_f < 45^o$. The data are, of course, symmetric about $\psi_f = 45^o$.

The introduction of a sidewise velocity component is seen in figure 8(b) to have a detrimental effect on the stability of the model with soft side shocks. A region of instability now exists whereas no instabilities were found in previous tests (figs. 6(b) and 7(b)). In all cases, however, the stability is better than that obtained for the model with equal-force shocks under similar landing conditions (fig. 8(a)). For $\psi_f = 90^o$, the soft shock absorbers are alined with the downhill slope as well as with the flight path.

Yawed Cross-Slope Landings

Stability profiles are shown in figures 9(a) and 9(b) for approach conditions identical to those in figures 8(a) and 8(b) with the exception that the flight path is now 30^o to the right of the direction of downhill slope. Again, the vertical component of the impact velocity is plotted as a function of the angle of yaw relative to the flight path. In figure 9(a) the stability profile for the model with equal-force shocks is seen to encompass approximately the same range of vertical impact velocities as in figure 8(a) where the model was launched directly downhill. However, the yaw conditions for maximum and minimum stability are different. In the downhill landing, the approach resulting in the most stable landing was that with two opposite feet alined with the flight path ($\psi_f = 0^o$ and 90^o). For the 30^o cross-slope landing, this approach is seen to be the least stable. The peaks in the landing profile at $\psi_f = -70^o$, -30^o, 20^o, and 60^o are associated with landings in which the center of gravity passes over one foot while the model overturns, whereas at intermediate angles the model pivots about a pair of feet during the latter stages of overturning.

The stable data point at $\psi_f = 0^o$ and $V_V = 3$ ft/sec (0.91 m/sec) is in conflict with the unstable data point of figure 6(a) at $\alpha_S = 30^o$ and $V_V = 3$ ft/sec (0.91 m/sec). It should be noted, however, that these two landings, as well as many others in the series, were marginal in that the model nearly balanced on two feet before falling one way or the other. It is possible, in such cases, that a slight misorientation of the model at impact would suffice to change its stability.

The effect of the soft side shock absorbers on landing stability for yawed cross-slope approaches may be observed by comparison of figure 9(b) with figure 9(a). As in the downhill approaches, the soft side shocks are seen to improve the landing stability at all values of ψ_f. Within the limitations of the test apparatus it was not possible to overturn the model from $\psi_f = -30^o$ to $\psi_f = 80^o$.

Additional Considerations

For the configuration with soft side shocks, there are, essentially, only two gear assemblies to absorb the kinetic energy of the vehicle compared to four for the current LM concept. It would, therefore, appear that the strut stroke might become excessive and present a clearance problem for the rocket nozzle. It should be noted, however, that in the current LM design the absorber force during the initial one-third of the available stroke is approximately one-half of the force during the remainder of the stroke, with the result that the total stroke and clearance for the current LM concept would be approximately the same as that for the early LM design modified with soft side shocks.

The chief constraint imposed by the use of soft side shocks is the limitation on sidewise velocity, not due to any degradation of landing stability but rather due to limited energy-absorption capabilities if the vehicle should fly sidewise into a hill or other obstacle.

CONCLUDING REMARKS

On the basis of the results presented herein, it is evident that the simple concept of using soft shock absorbers in the side landing-gear assemblies of a four-legged vehicle can significantly improve the landing stability if the vehicle is roughly alined with the flight path at touchdown. For touchdowns at large yaw angles, the landing stability obtained with soft side shock absorbers was at least as good as that obtained with four equal-force shock absorbers.

Langley Research Center,
National Aeronautics and Space Administration,
Langley Station, Hampton, Va., May 3, 1968,
124-08-04-13-23.

REFERENCES

1. Walton, W. C., Jr.; Herr, R. W.; and Leonard, H. W.: Studies of Touchdown Stability for Lunar Landing Vehicles. J. Spacecraft, vol. 1, no. 5, Sept.-Oct. 1964, pp. 552-556.

2. Herr, Robert W.; and Leonard, H. Wayne: Dynamic Model Investigation of Touchdown Stability of Lunar-Landing Vehicles. NASA TN D-4215, 1967.

3. Walton, William C., Jr.; and Durling, Barbara J.: A Procedure for Computing the Motion of a Lunar-Landing Vehicle During the Landing Impact. NASA TN D-4216, 1967.

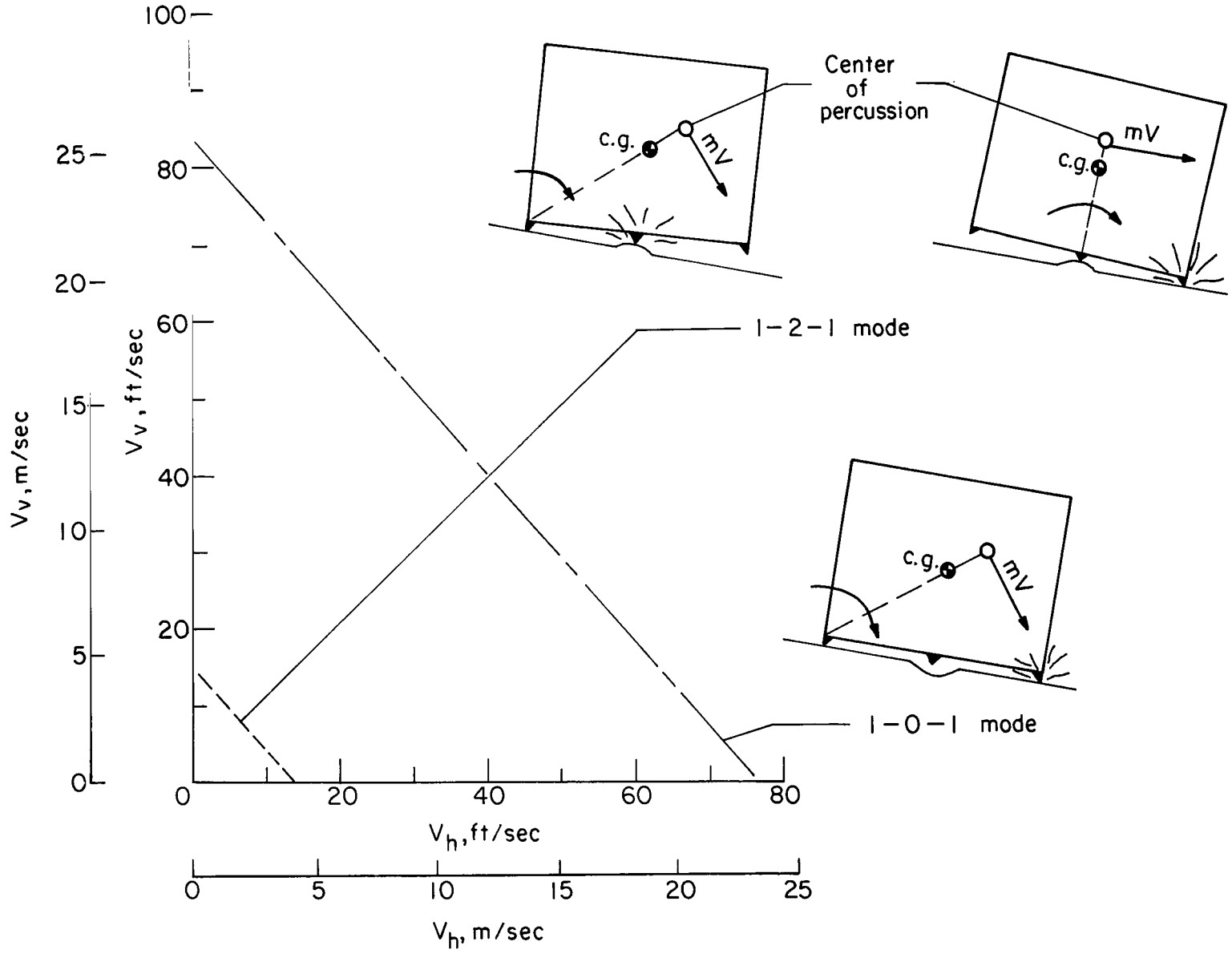

Figure 1.- Two-dimensional rigid-body stability. $\sigma = 10^0$.

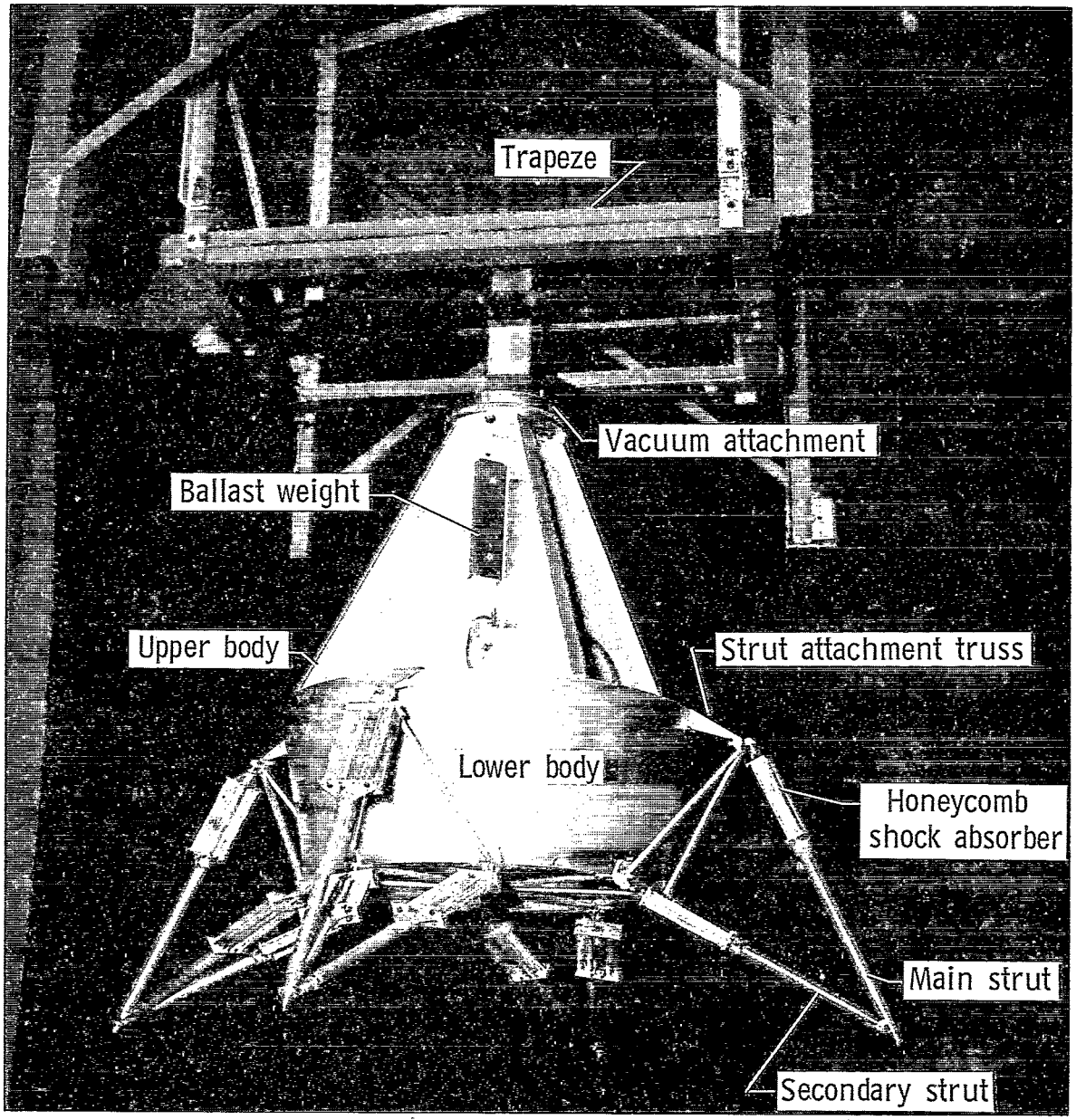

Figure 2.- One-sixth-scale model.

L-64-8103.1

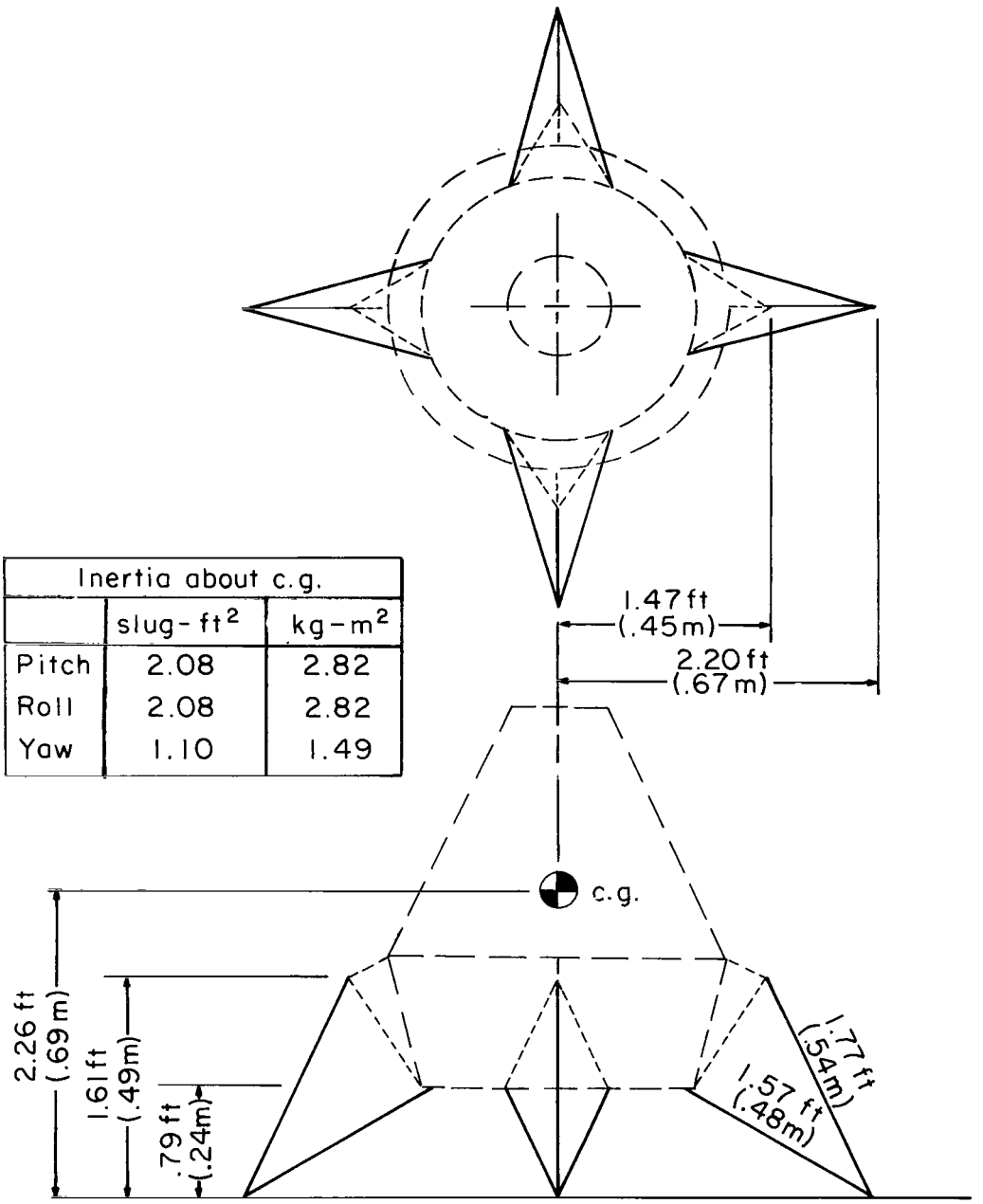

Figure 3.- Dimensional, mass, and inertial properties of 1/6-scale model. Mass, 1.66 slugs (24.22 kg).

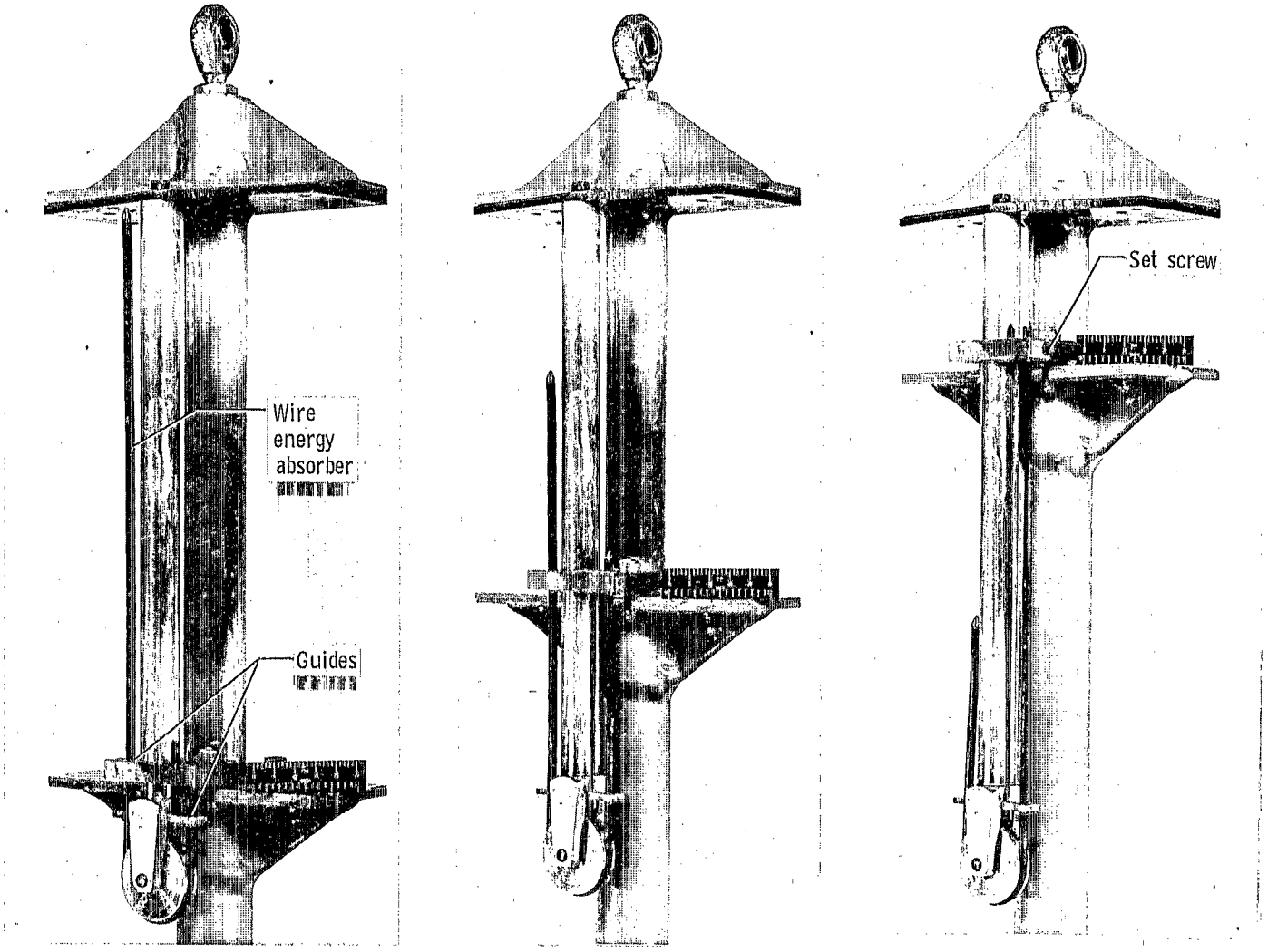

(a) Fully extended.

(b) Partially stroked.

(c) Fully stroked.

Figure 4.- Wire energy absorber.

L-68-892

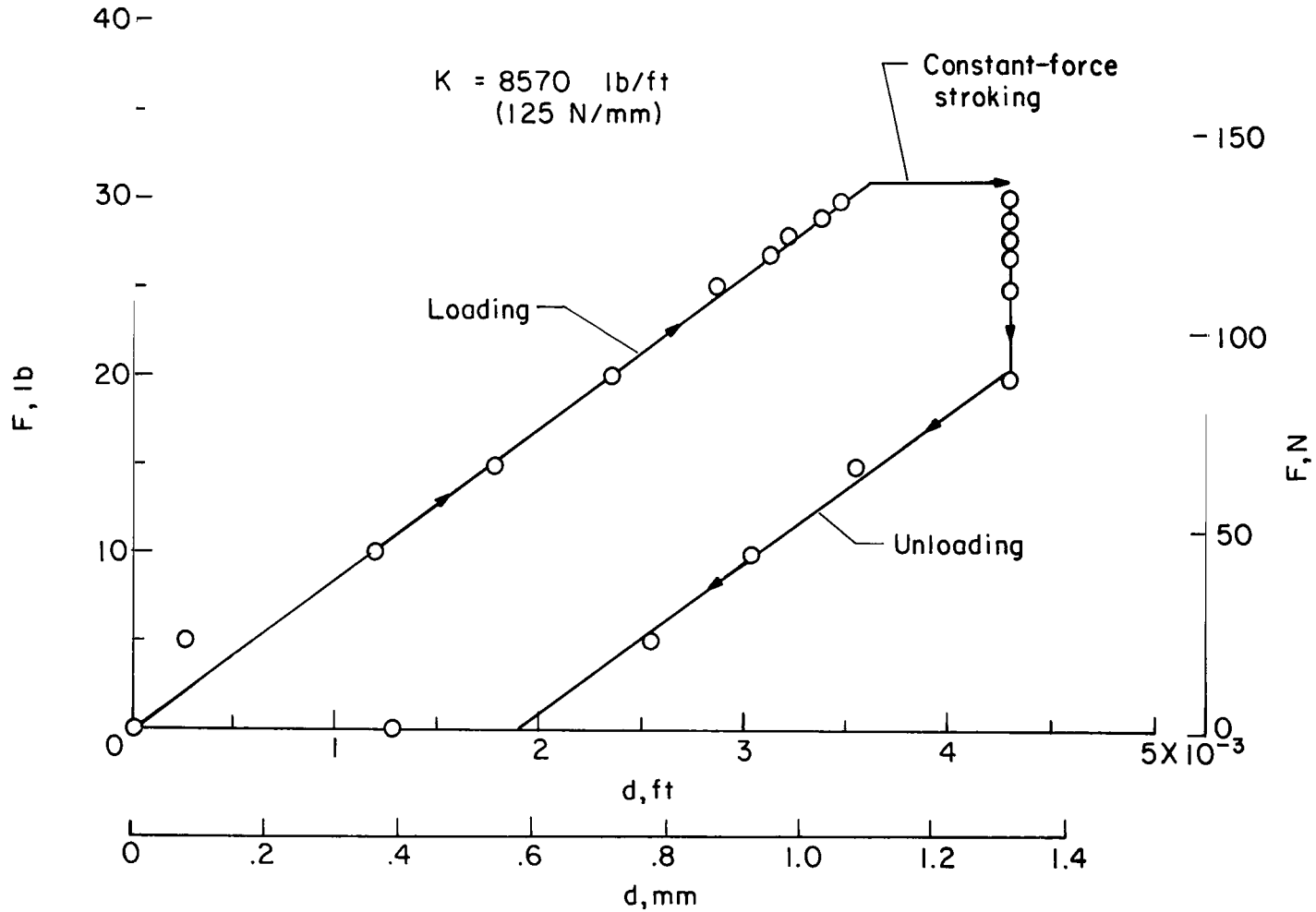

Figure 5.- Force-deflection curve of strut with wire energy absorber.

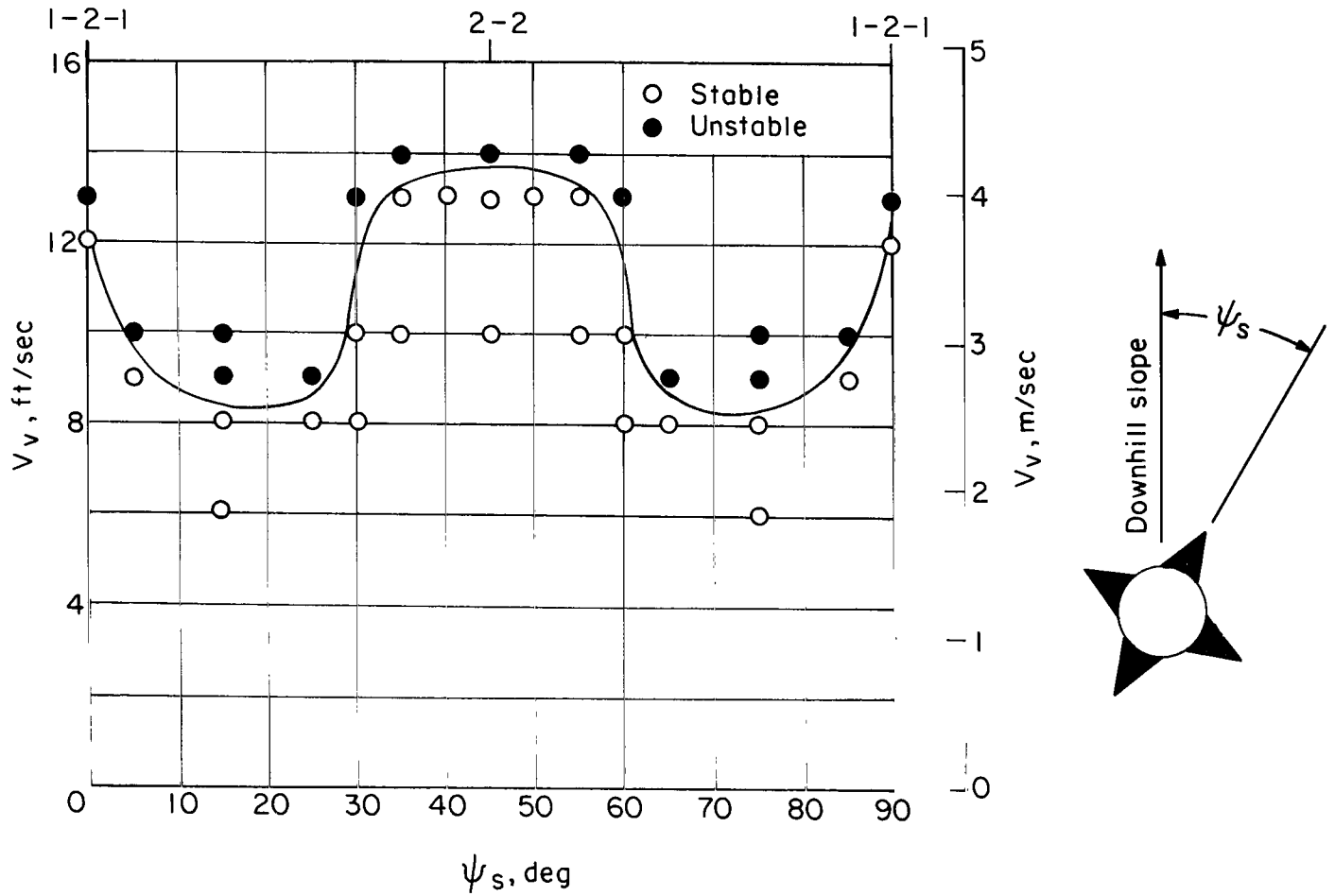

(a) Equal-force shocks. $V_h = 0$; $\sigma = 10^0$.

Figure 6.- Vertical impact stability indicated by vertical velocity as a function of yaw orientation relative to direction of slope.

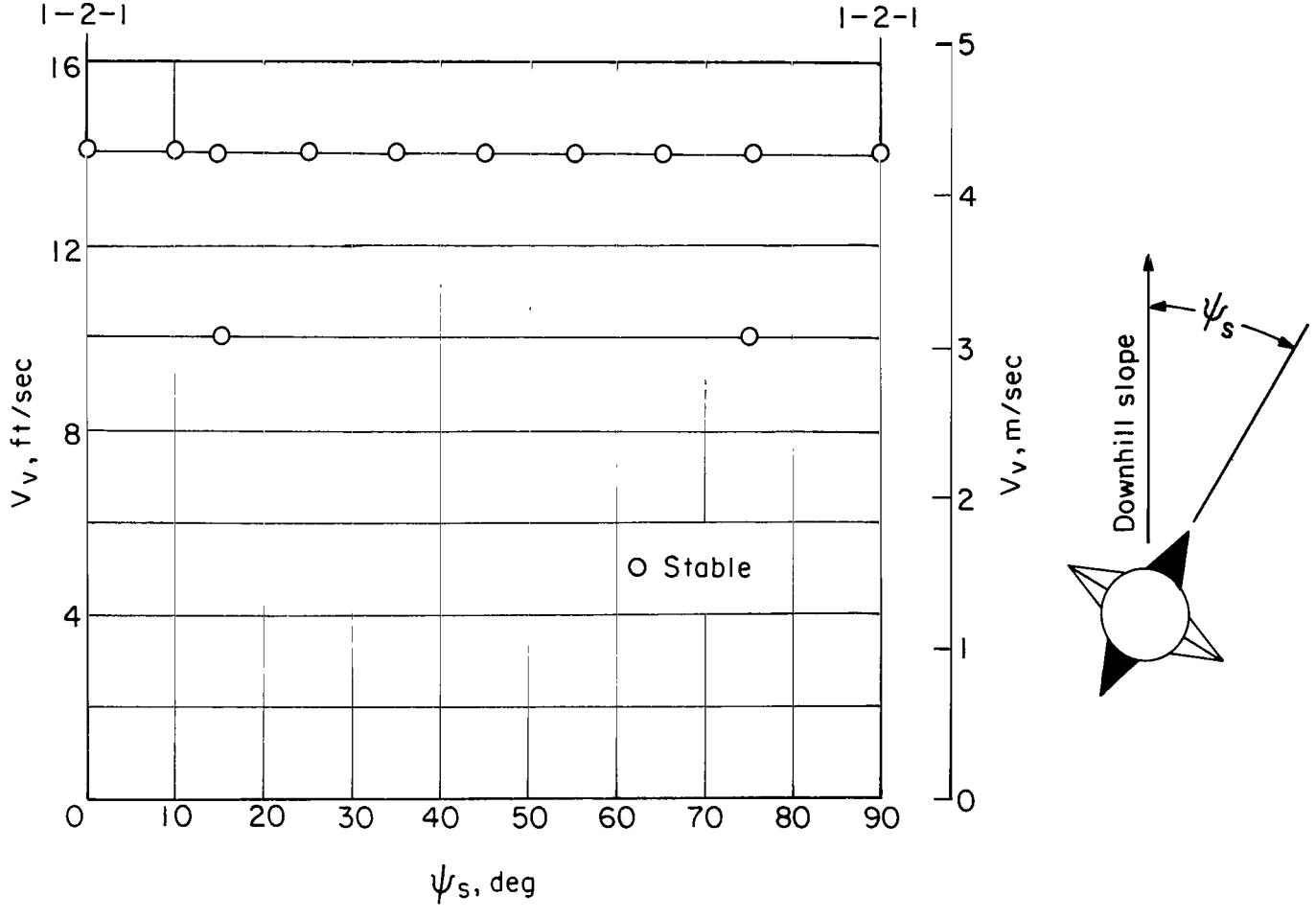

(b) Soft side shocks. $V_h = 0$; $\sigma = 10^0$.

Figure 6.- Concluded.

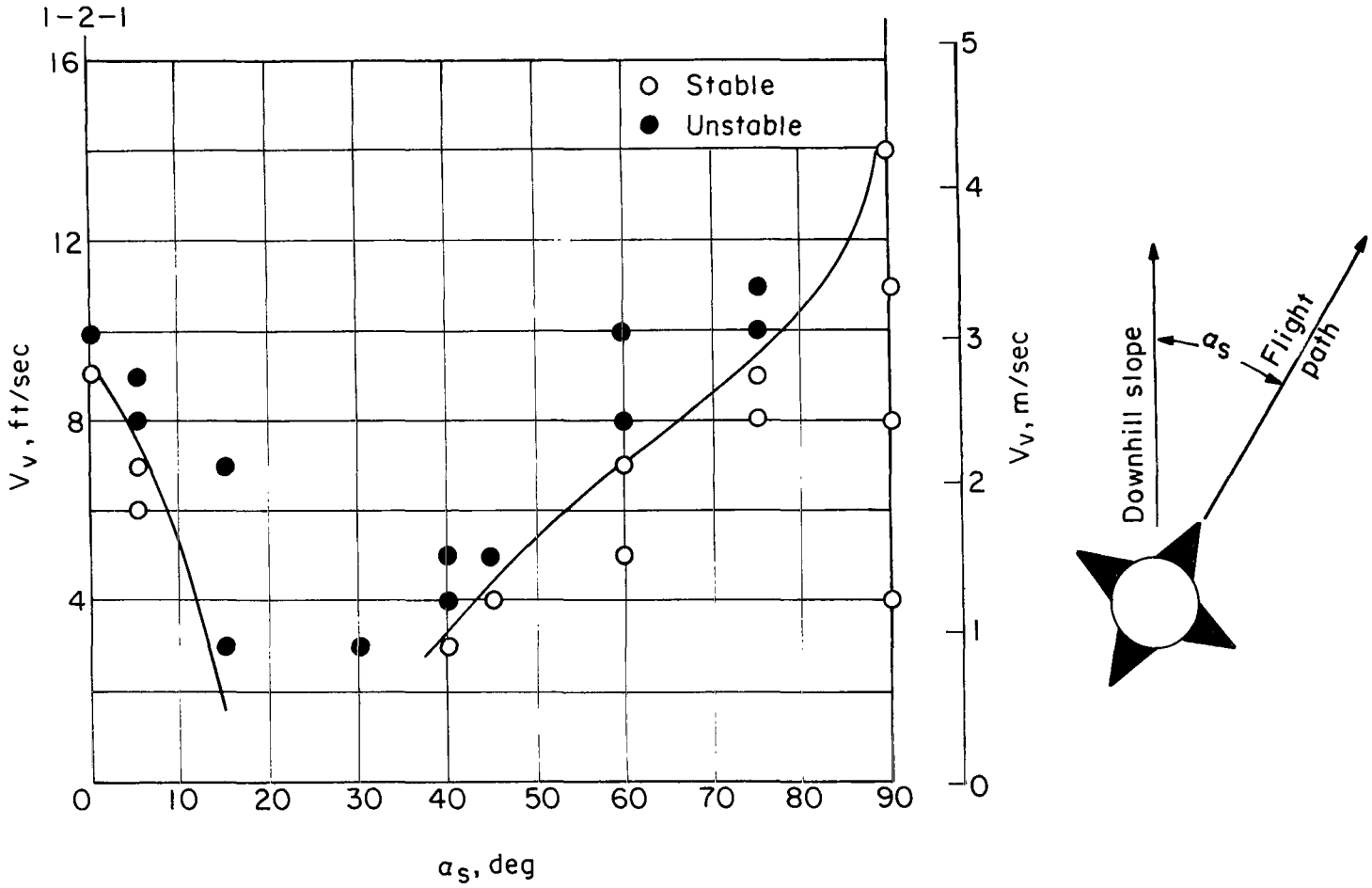

(a) Equal-force shocks. V_h = 5 ft/sec (1.52 m/sec); $\psi_f = 0^0$; $\sigma = 10^0$.

Figure 7.- Cross-slope stability indicated by vertical velocity as a function of cross-slope angle.

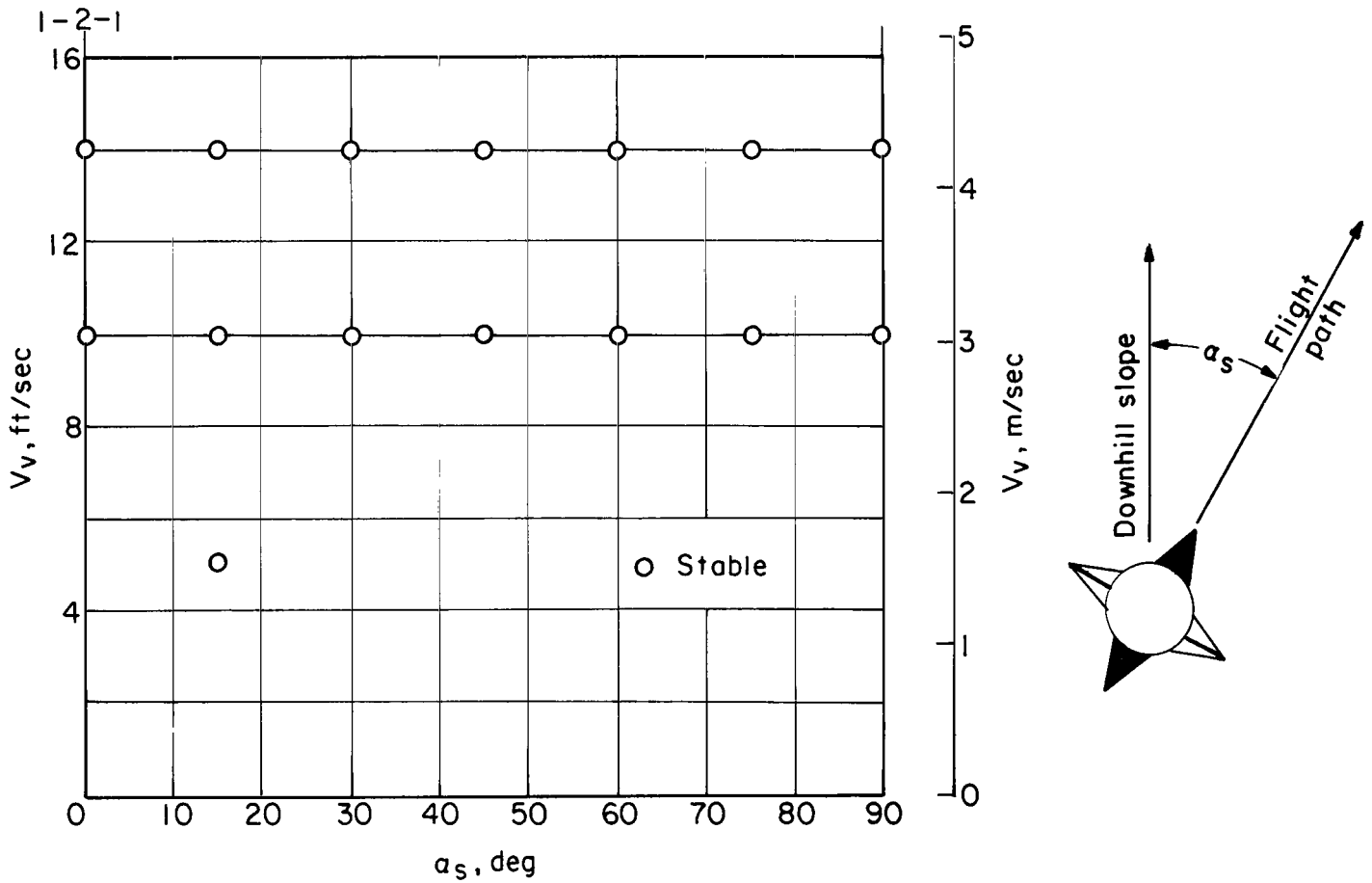

(b) Soft side shocks. V_h = 5 ft/sec (1.52 m/sec); $\psi_f = 0^0$; $\sigma = 10^0$.

Figure 7.- Concluded.

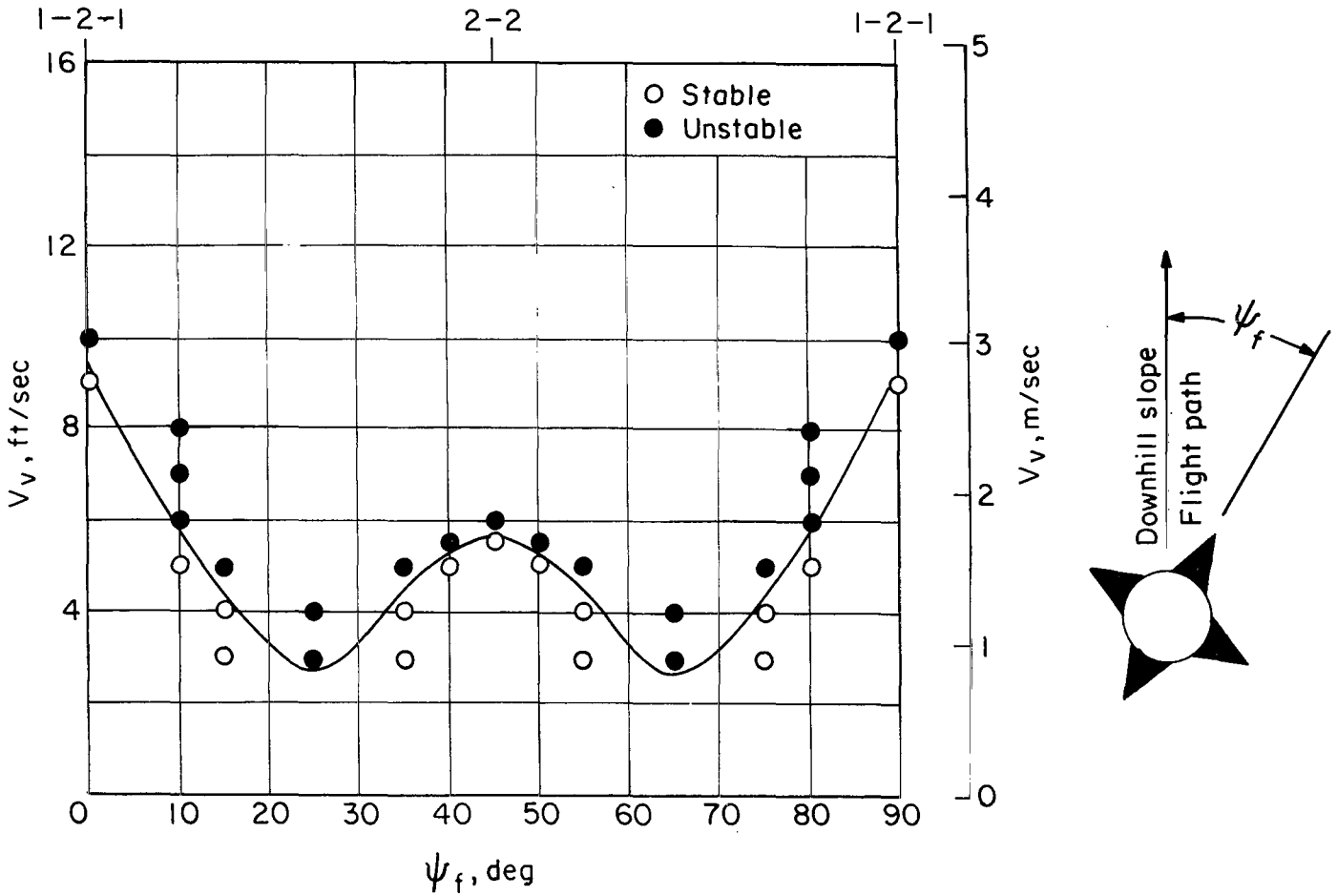

(a) Equal-force shocks. V_h = 5 ft/sec (1.52 m/sec); $\alpha_s = 0^0$; $\sigma = 10^0$.

Figure 8.- Yawed downhill stability indicated by vertical velocity as a function of yaw orientation relative to flight path.

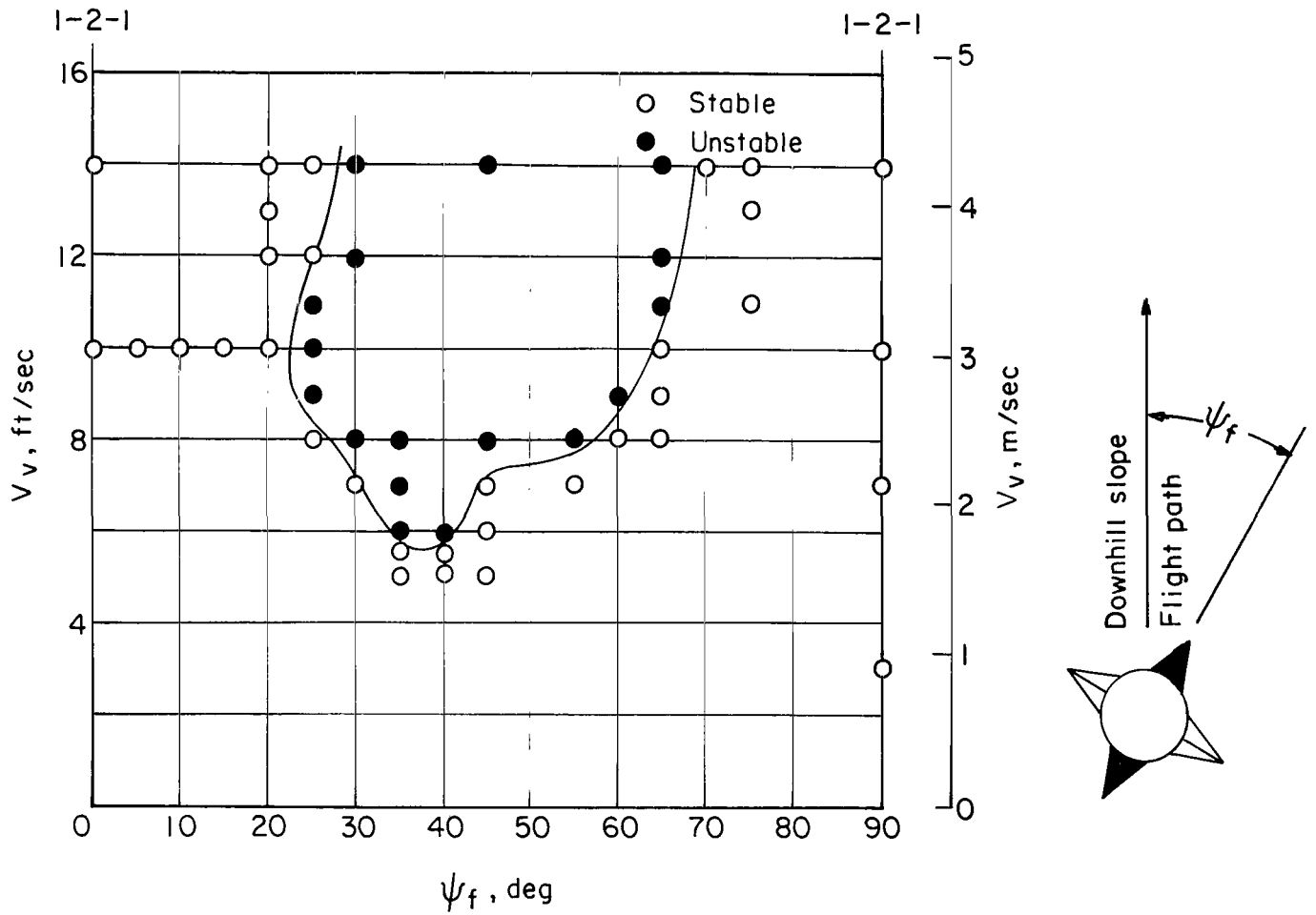

(b) Soft side shocks. V_h = 5 ft/sec (1.52 m/sec); $\alpha_s = 0^0$; $\sigma = 10^0$.

Figure 8.- Concluded.

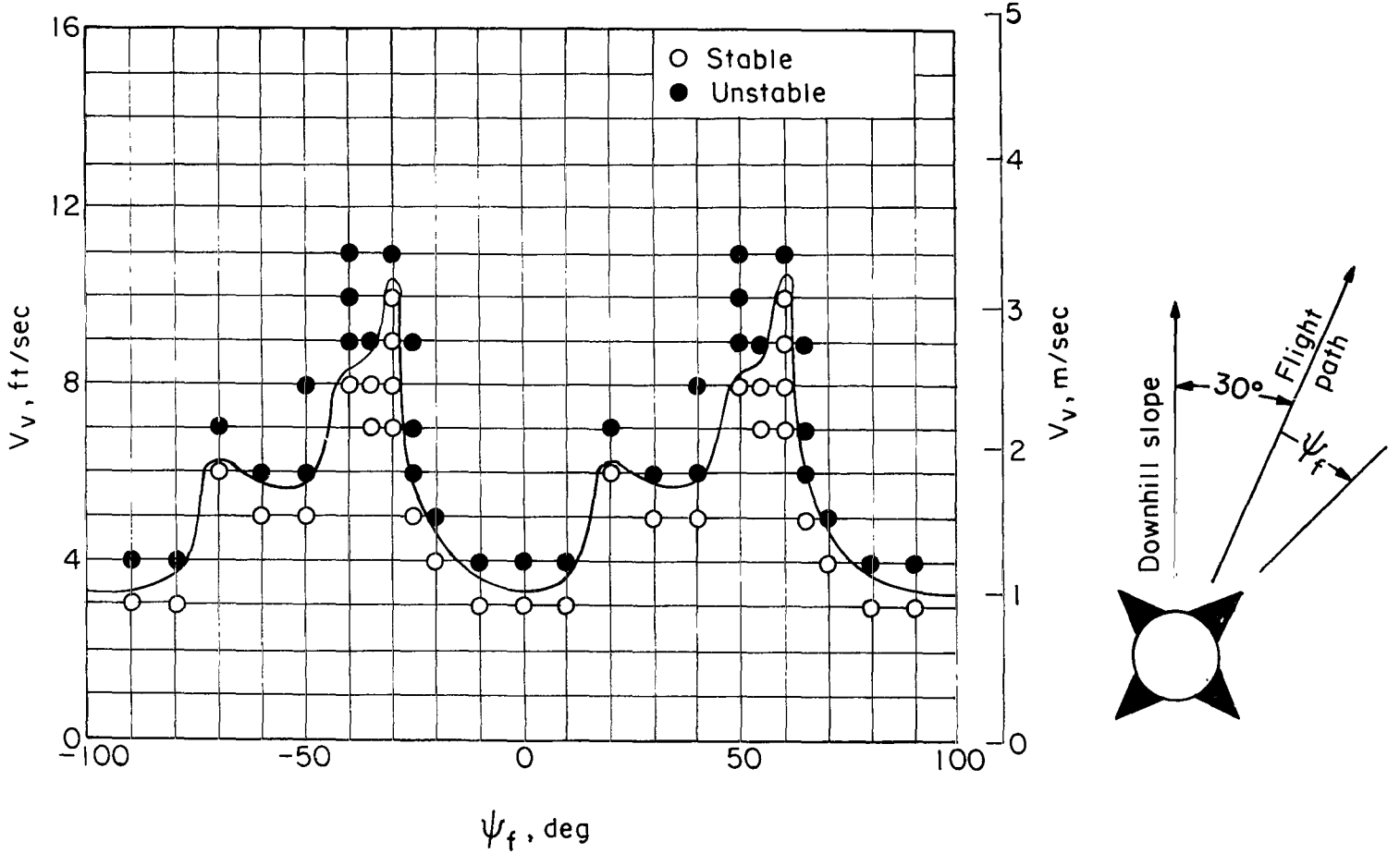

(a) Equal-force shocks. V_h = 5 ft/sec (1.52 m/sec); α_s = 30°; σ = 10°.

Figure 9.- Yawed cross-slope stability indicated by vertical velocity as a function of yaw orientation relative to flight path.

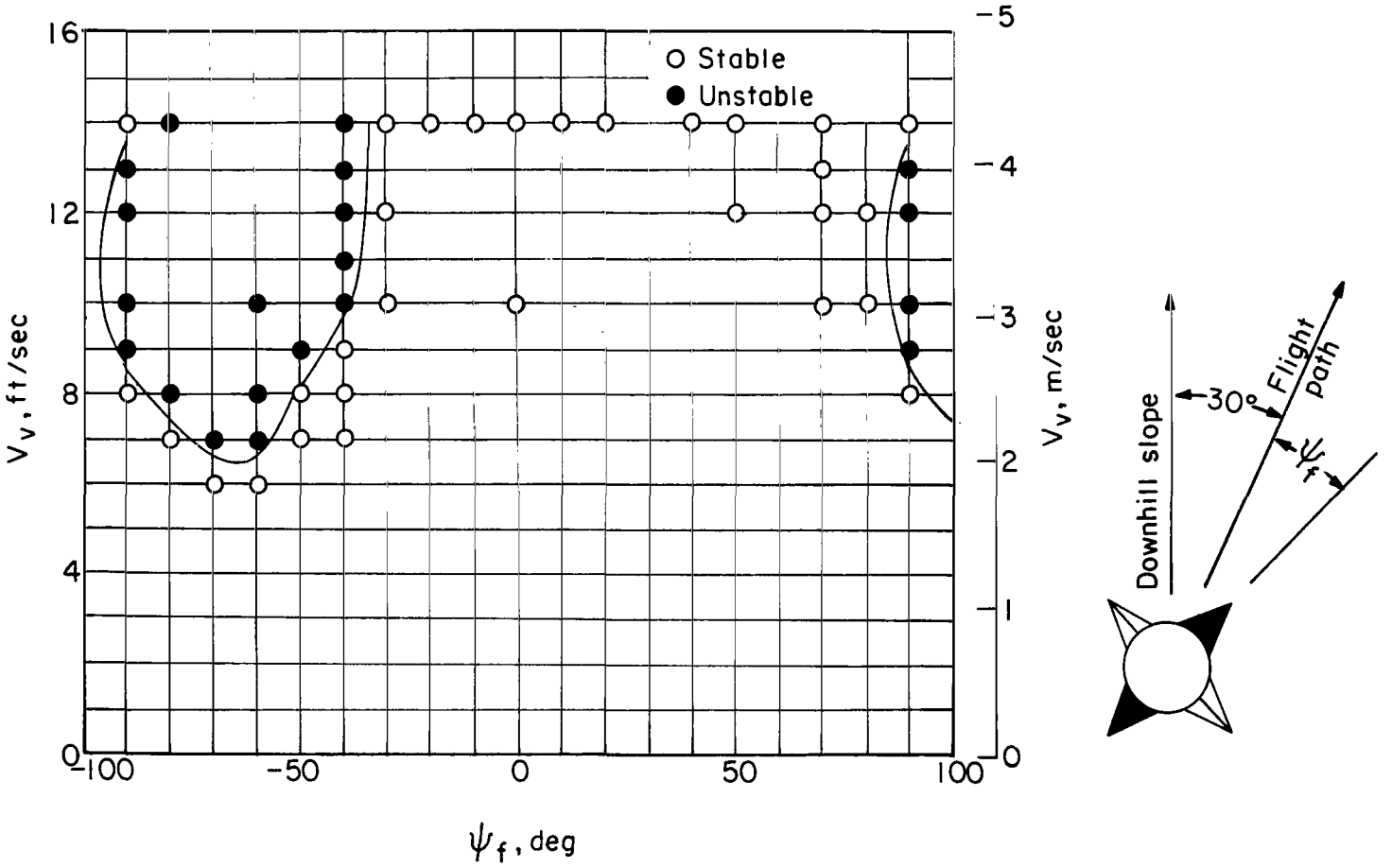

(b) Soft side shocks. V_h = 5 ft/sec (1.52 m/sec); $\alpha_s = 30^0$; $\sigma = 10^0$.

Figure 9.- Concluded.

NATIONAL AERONAUTICS AND SPACE ADMINISTRATION
WASHINGTON, D.C. 20546
OFFICIAL BUSINESS

FIRST CLASS MAIL

POSTAGE AND FEES PAID
NATIONAL AERONAUTICS AND
SPACE ADMINISTRATION

POSTMASTER: If Undeliverable (Section 158 Postal Manual) Do Not Return

"The aeronautical and space activities of the United States shall be conducted so as to contribute . . . to the expansion of human knowledge of phenomena in the atmosphere and space. The Administration shall provide for the widest practicable and appropriate dissemination of information concerning its activities and the results thereof."

—NATIONAL AERONAUTICS AND SPACE ACT OF 1958

NASA SCIENTIFIC AND TECHNICAL PUBLICATIONS

TECHNICAL REPORTS: Scientific and technical information considered important, complete, and a lasting contribution to existing knowledge.

TECHNICAL NOTES: Information less broad in scope but nevertheless of importance as a contribution to existing knowledge.

TECHNICAL MEMORANDUMS: Information receiving limited distribution because of preliminary data, security classification, or other reasons.

CONTRACTOR REPORTS: Scientific and technical information generated under a NASA contract or grant and considered an important contribution to existing knowledge.

TECHNICAL TRANSLATIONS: Information published in a foreign language considered to merit NASA distribution in English.

SPECIAL PUBLICATIONS: Information derived from or of value to NASA activities. Publications include conference proceedings, monographs, data compilations, handbooks, sourcebooks, and special bibliographies.

TECHNOLOGY UTILIZATION PUBLICATIONS: Information on technology used by NASA that may be of particular interest in commercial and other non-aerospace applications. Publications include Tech Briefs, Technology Utilization Reports and Notes, and Technology Surveys.

Details on the availability of these publications may be obtained from:

SCIENTIFIC AND TECHNICAL INFORMATION DIVISION

NATIONAL AERONAUTICS AND SPACE ADMINISTRATION

Washington, D.C. 20546